AXIAL FAN BEARING SYSTEM VIBRATION ANALYSIS

Dr. Assim H Yousif Dr. Muawafak A Tawfik Dr. wafa Abd Soud

Mechanical Engineering Department, University of Technology, Baghdad.

ABSTRUCT

Rotating fan shaft system was investigated experimentally and theoretically to study its dynamic performance. The type of oil used for the bearing was taken in consideration during the experimental program .Three types of oil were used, SAE 40, SAE 50 and degraded oil. During the experiments, the fan blades stagger angle was changed through angles (20˚, 30˚, 40˚, and 50˚). The shaft rotational speed also changed in the range of (0-3000 rpm). All these parameters have investigated for two cases (balanced and unbalanced fan). The performance parameters of the fan were found experimentally by measuring the fan, volume flow rate, Reynolds and Strouhal numbers, efficiency and pressure head. Analytical part was also represented to prepare the prediction of fan system dynamic performance. The aerodynamic forces and moments of each blade were also predicted to obtain the rotor dynamic future. Experimentally and theoretically the critical fan speed was obtained in the x and y direction for different lubricant oil viscosities and shaft rotational velocities for balanced and unbalanced fan. Analysis of the vibrational response gave important information about the dynamic performance of fan rotating system. Acceptable agreement was found between analytical and experimental results.

الخلاصة

تم اختيار منظومة عمود إدارة مروحة دوارة تجريبيا ونظريا لدراسة أدائها الديناميكي .لقد تم أخذ نوع الزيت المستخدم في تزييت المساند بنظر الاعتبار في برنامج الاختبار التجريبي. ثلاثة أنواع من زيوت التزييت استخدمت SAE 40 وSAE 50 وزيت منتهي الصلاحية .خلال التجارب تم تغيير زاوية الريشة أربع مرات وهي 20° ، 30° ، 40° و 50°. أن سرعة المحور الدوار تتغير من صفر إلى 3000 دورة بالدقيقة. كل هذه المعالم اختبرت لحالتي المروحة المتوازنة والغير متوازنة. إن معالم أداء المروحة تم تحديده بقياس معدل التدفق الحجمي لجريان الهواء ورقمي رينولدز وستروهل وكفاءة المروحة وارتفاع الضغط . كذلك تم انجاز الجزء النظري للتنبؤ عن الأداء الديناميكي للمنظومة للحصول على ديناميكية الدوار . تجريبيا ونظريا تم الحصول على السرعة الحرجة للمروحة في اتجاهي المحورين X و Y لمختلف أنواع الزيت (مختلف اللزوجة)ومختلف سرع الدوران لحالتي التوازن وعدم التوازن.التحليل النظري لاستجابة الاهتزاز أعطت معلومات مهمة للأداء الديناميكي لمنظومة الدوران. كما وجد أن هناك توافق مقبول بين النتائج النظرية والعملية.

Dr. Assim H Yousif
Dr. Muawafak A Tawfik
Dr. wafa Abd Soud

INTRODUCTION

In the design study of turbo-machinery, performance and rotor dynamic considerations are often in compromise. The rotor performance usually desires to maximize the volume flow rate and the pressure, and minimize the fluid energy losses, though a machine of limited size and weight. This generally suggests high shaft speed, and multiple stages. All of these features tend to create rotor dynamic problems. The goal of increasing the efficiency of machines is essential for their development. Engineers and Scientists work to reach ways and method to guide the designers to develop new designs to reach this goal. They develop machine designs in order to prevent the operations errors and to predict them early.

The characterization of these errors and their causes is essential in the maintenance process in order to prevent the unexpected failure in these machines. These predicted errors can be found by using simple measuring equipments for vibrations and also by analytical methods. The causes of these vibrations can be predicted and the pre-prevented solutions can be found, which in fact would decrease the cost and increase the efficiency, which is the goal, and these are crucial in industry. This research,deals with the prediction of these errors, in order to reach this goal a fan rotor bearing casing system has been built up and vibration measuring equipments have been used.

The vibration in this system can be due to one of the following variables or combinations of them:

1. Changing the stagger angles.
2. Degradation of oil used.
3. Changing revolution speed.
4. Unbalance in fan or rotor shaft (crack, failure and dirt).

In addition to that, in the current research numerical solution, used to create, develop and modify computer software to give the required results for the dynamic response for each system.

ROTOR DYNAMIC FUTURE

All fans generate some vibration. They continuously rotate and since nothing is perfect, cyclic forces must be generated .Its only when vibration reaches certain amplitude that may be call "bad". Vibration may just be an indicator of some problem with a mechanism, or it may be cause of other problem .High vibration can breakdown lubricants in the bearings and, in addition may cause metal fatigue in the bearings. Excessive vibration can cause fasteners to loosen or can cause fatigue failure of structurally loaded components. Also vibration can be transmit into adjacent areas and interfere with precision processes, or create an annoyance for people.

Thus, experimental and numerical results can be used to analyze the vibrating signal (amplitude), and to predict the causes of these vibrations. The design of successful and reliable turbomachine requires cooperation and compromises between the two descriptions. From a rotor dynamic standpoint of view, the successful design of a turbomachine involves [**Tohn,1988**]. Avoiding critical speeds, if possible and minimizing dynamic response at resonance, if the critical speed is traversed. Minimizing vibration and dynamic load transmitted to machine structure through out the operating speed range. Avoiding turbine or compressor blade tip or seal rub, while keeping tip clearance and seals as tight as possible to increase the efficiency. Avoiding rotor dynamic instability and avoiding torsion vibration resonance or torsion instability of the drive train system.

EXPERAMENTAL SET- UP

The axial fan used in the test rig is usually used in airconditioning system and industry. The fan is of ten blades aerofoil section [NACA 0021], each blade span is (120.8) mm, root chord is (61.7) mm, tip cord of (46.1) mm, leading edge twist angle is (14°), trailing edge twist angle is (zero) °. The fan located close to the shaft end. The fan blades material is (AL–Cast–Alloy) of density (2650 kg/m3) and a young modules equal to 7600 kgf/mm^2 [**R.N.Peter, 1998**]and each blade weights (0.196kg) .The stagger angles of the blade can be changed during the test from (20° to 50°) by steps of (10°).The disk rotor diameter is (400 mm), maximum blade thickness is (5.15 mm),i.e. located at 20%, chord located from the leading edge. The fan duct diameter is (404.8 mm), thus the tip clearance is 2.4 mm according to the data given in [**L.Neuhaus, 2002**] .The tip clearance can be varied by exchanging the casing segments using adjustable screw maintained on the outer diameter of the duct to take into account the unbalance effect of the fan during the experimental test. Figure (1) shows the fan photograph. According to [**S.L.Dixon, 1978**] which gave the power required calculation procedure a 1.5 kW motor is used to derive the fan.

The rotor system consists of a rotor shaft carrying the axial fan and two journal bearings. The bearings were selected according to the maximum rotor shaft speed (3000 rpm), using the information given in [**R.N.Peter, 1998**].The motor speed was controlled by using invertors.

Two accelerometer in the x and y directions were mounted on the journal bearing by means of epoxy resin so that the surfaces were kept flat and smooth where the sensor is located as in figure (2).

Laser tachometer with the SBS Portable Balancer is used to measure relationship between measured vibration and the spinning rotor. This information is important in determining position of balance weight.

ASSUMPTION

For the sake of analysis, the following assumptions are adopted:

1. Axial fluid flow is constant along the blade.
2. Aerodynamic forces which are cased by air flow act on the center line of the blade surface.
3. Assume incompressible fluid flow.
4. Coefficients of damping and stiffness are to be changed during the rotation speed in the journal bearing.

For the present purpose of investigation, the system can be reduced into two coupled beams. The shaft and the casing are treated as a simply supported beam [**M.A.Tawfik, 1996**] rested between two bearing and supporting structure as shown in Figure (3).

SYSTEM STATE VECTOR

The state vector at any point in the system (Fan blade –Disk – Rotor –Bearing) is the state vector of the station (i). There are two state vectors, one to the left $[Z]_i^L$, and the other to the right $[Z]_i^R$ contains two displacement component (y) and (ϕ), that is the deflection and mode shape , also associated state with these displacements are internal force (V) and moment (M), i.e. shear force and bending moment respectively . The state vector $[Z]_i$ can be written as indicated in [**M.A.Tawfik, 1996**] and [**I.Wattar, 2000**].

$\{Z\}_i$ = { Z_S X_S Y_S ϕ_{ZS} ϕ_{XS} ϕ_{YS} M_{ZS} M_{XS} M_{YS} V_{ZS} V_{XS} V_{YS} Z_C X_C Y_C ϕ_{ZC} ϕ_{XC} ϕ_{YC} M_{ZC} M_{XC} M_{YC} V_{ZC} V_{XC} V_{YC} 1 } (1)

Where X, Y and Z represent the deflection in x, y and z respectively,

ϕ_{ZS} is the torsion angle about Z-axis, 4

ϕ_{XS} , ϕ_{YS} are the components of the mode shape in x, y axis,

M_Z is the torsion moment about Z-axis, M_X and M_Y are the bending moment about x and y axis'

V_Z is the axial force in Z-direction,

V_X and V_Y are the shear force in x and y directions, and subscripts C and S are indicated casing and rotor respectively.

UNBALANCE FORCES

Unbalance forces is defined as the allowance for a circumferential change in its position. It is a kind of excitation for the system. The unbalance force component [**M.A.Tawfik, 1996**and **Barth, 1976**] according to Figure (4) may be written as;

$$\Omega^2 U_y = \Omega^2 U^*_y \cos\Omega t - \Omega^2 U^*_x \sin\Omega t \quad (2)$$

$$\Omega^2 U_x = \Omega^2 U^*_x \cos\Omega t + \Omega^2 U^*_y \sin\Omega t \quad (3)$$

While as a complex function

$$\Omega^2 \overline{U}_y = \Omega^2 U^*_y + j\Omega^2 U^*_x \quad (4)$$

$$\Omega^2 \overline{U}_x = \Omega^2 U^*_x - j\Omega^2 U^*_y \quad (5)$$

POINT MATRIX (MASS ELEMENT MATRIX):

There are four cases for the point matrix. These cases cover all the possible arrangement at any station along the system as shown in figure (5)and they overall used to analyze the theoretical solution .

1- Lumped mass at the station (i):

a- lumped mass on rotor and casing [**M.A.Tawfik, 1978**]

b- Lumped mass on rotor and imaginary lumped mass on casing.

2- Bearing station

3- Pulley at the shaft and lumped mass on the casing.

4- Branch of fan blade.

There are two kinds of point matrix one where there are two real masses of casing and shaft as in Figure (6) and another one where there is imaginary part at the casing and real part in shaft's mass as in Figure (7). For the case(2)(bearing station)take the equilibrium of journal bearing in X and Y-direction then find the deflection ,slop, shear force and bending moment for this case as in figure (8).

Where

$$[QQ] = [GG][W]^{-1}[HH]$$

$$[DD] = [GG][W]^{-1}[RR]$$

$$[D]_{2\times2} = [ss] - [RR][W]^{-1}[RR] \quad ,$$

and $[Q]_{2\times2} = [RR][W]^{-1}[HH] - [RR]$

Where

$$[GG] = \begin{bmatrix} K_{YY} + j\Omega_Y c_{YY} & K_{YX} + j\Omega_X c_{YX} \\ K_{XY} + j\Omega_Y c_{XY} & K_{XX} + j\Omega_X c_{XX} \end{bmatrix}$$

Where

$$[ss] = \begin{bmatrix} -\Omega^2 m_c + k_{cyy} + j\Omega c_{cyy} + Z_{yy} & k_{cyx} + j\Omega c_{cyx} \\ k_{cxy} + j\Omega c_{cxy} & -\Omega^2 m_c + k_{cxx} + j\Omega c_{cxx} + Z_{xx} \end{bmatrix}$$

where

$$[W]=\begin{bmatrix} -\Omega^2 m_p+k_{cyy}+k_{yy}+j\Omega c_{cyy} & k_{cyx}+k_{yx}+j\Omega c_{cyx}+j\Omega c_{yx} \\ k_{CXY}+k_{xy}+j\Omega c_{CXY}+j\Omega c_{xy} & -\Omega^2 m_p+k_{cxx}+k_{xx}+j\Omega c_{cxx}+j\Omega c_{xx} \end{bmatrix}$$

$$[HH]=\begin{bmatrix} -\Omega^2 m_p+k_{cyy}+j\Omega c_{cyy} & k_{cyx}+j\Omega c_{cyx} \\ k_{cxy}+j\Omega c_{cxy} & -\Omega^2 m_p-k_{cxx}+j\Omega c_{cxx} \end{bmatrix}$$

$$[RR]=\begin{bmatrix} k_{cyy}+j\Omega c_{cyy} & k_{cyx}+j\Omega c_{cyx} \\ k_{CXY}+j\Omega c_{cxy} & k_{cxx}+j\Omega c_{cxx} \end{bmatrix}$$

In case (4)The point matrix take in to consideration the effect of branch because of the dynamic load and gyroscope moment effect on the brunch system (moving blade)and the difference between the magnitudes properties of mass element (i).For the point matrix in the direction of the system will be as shown in figure (9).

COMPUTER PROGRAM CODE

A computer program written in FORTRAN 77 has been developed to embrace the theoretical work. The program adopted Figure (3) as a lumped masses distributed uniformly with circular shapes, negligible weight, having rigidity equal to the actual systems rigidity. The program takes into consideration the effect of, gyroscopic moment, shear force, moment of inertia for rotor and casing, Stiffness and damping coefficients of journal bearing and the Branch of the fan blade. To minimize the error and to enhance the accuracy of the results, non- dimensional terms are implemented.

The fan blade branch and journal bearing system have been reduced to a single matrix for the purpose of the solution .The rotor shaft has been divided in to (33) stations of masses and (32) of massless sections .The program has the ability to find the deflection, mode shape, shear force and moment for each station along the shaft and casing for a rang of speed (0-3000) rpm

The program was developed for the rotor, casing and branch system .In order to evaluate the final matrix, the point matrices are multiplied by the field matrices and boundary conditions are applied for the system to find the state vector in three dimensions along the system for every rotating speed and for different stagger angle and different oil viscosity in the journal bearing.

Performance Characteristic of the Fan

Results were obtained for a range of flow rate and various stagger angels of the fan blade at three different kinematics viscosity of oil used in bearing system, so that, the fan performance data could be generated. Sample of the fan performance characteristics is illustrated in Figure (10) as plots of qualitative performance curve for a typical fan stagger angle [40º] and for lubricant oil SAE 40 (Kinematics Viscosity =140 c.s), the efficiency curve leans more to the right; the head tends to decrease with flow rate increasing. The fan efficiency drops off rapidly for volume flow rate higher than that at the best efficiency point. The net head curve also decreases continuously with flow rate, although there are some wiggles. If the fan operated below its maximum efficiency point, the flow might be noisy and unstable which indicates that the fan may be oversized (large than necessary) [**Franklyn, 2002**]. For this reason it is usually best to run a fan at, or slightly above its maximum efficiency point.

In the duct fan, a vortex shedding will appear in the flow down stream of the fan in addition to unsteady flow which can be represented by non-dimensional group, Strouhal number(St). Figure (11) shows a non-dimensional numbers, Reynolds number (Re) and (St) of the duct fan.

(St) represents the characteristic dimension of the body (D) times the system frequency of vibrations (f) divided by the fluid free stream velocity (U∞). For axial fluid flow, the characteristic dimension taken as the outer diameter of the fan [**McGraw-Hill, 2006**], also the Re based on the outer diameter of the fan [**Franklyn, 2002**]. It can be seen from this figure, that at low stagger angle [20° low flow rate], the shedding frequency is fluctuating on the fan system ,due to the generation of forces on the fan structure .The vortex will be existed down stream of the fan [**Yunus, 2006**], and increased as the rotor speed increased .On the other hand, when using degraded oil (kinematics viscosity =117 c.s) at stagger angle equals (40º) and (50°) the value of strouhal no. is relatively high. At the stagger angle (30º), the vibration is at low values (St=0.5) and sharply increase to higher values (St=1.4) at Re=1.5x105. As Re increase the fluctuation behaviors of St and appeared to be more stable ranging between 1.32 and1.5. However, the St would seem to be higher at stagger angle (40°) and increase as the oil's viscosity increases, but at angle (50º), the vibration still be exist. However, these fluctuations are less than that for stagger angle (20°), but it is still high and become higher when using degraded oil. Due to swirl fluid downstream of the duct fan which leads to waste of kinetic energy and a high level of turbulence; this wasted kinetic energy partially reduced the level of the turbulence by using stator.

AMPLITUDE IN (X) AND (Y) DIRECTION:

Theoretical and experimental amplitude in X and Y directions for different system rotating speed, stagger angle and viscosity are indicated in figure (12). The remarkable point raised from this Figure is that the natural frequency occurs at the same speed in x and y directions and the amplitude in the x-direction higher than its values in the y-direction for the first appear of the natural frequency. At some rotating speed natural frequency appears in the x directions and disappears in the y direction. Also it can be seen that the amplitude in x and y decreased when stagger angle is increase. The behavior of the theoretical work is the same in the x and y directions with slight differences. The amplitude of vibration in the x-direction decreases as the stagger angle increases. The closeness between experimental and theoretical results are acceptable (0-19.2%). The difference in values of x and y directions amplitude demonstrate the difference in stiffness coefficients. While Figure (13) shows that many natural frequencies occurred with high viscosity figure of oil in journal bearing for the same range of rotor speed. Also some natural frequencies appear in x and disappear in y directions.

Figure (14) shows that the amplitude in x and y directions decreased as the stagger angle increased. Figures (15) and (16) show a comparison between the experimental and theoretical work for x and y amplitudes versus rotor speed for different stagger angle and oil viscosity. The main conclusion raised from these results is that the experimental and the theoretical results are close to each other except at stagger angle 40˚.

EFFECT OF UNBALANCE FORCE ON THE VIBRATION ANALYSIS

Two masses of (m1=8 gm, m2=16 gm) are replaced at a radius of 62 mm from the fan hub center line, to measure the effect of unbalance masses on the system response of the vibration at bearing station(21).

Figure (17) shows the amplitude in x-direction .It can be seen that the amplitude of vibration at balance force is small in magnitude and increases when the unbalance forces are increased. The maximum amplitudes in all the cases, Figure (18), occurred at a rotor speed (1339 rpm).The maximum amplitude appears at stagger angle 20º which is equal to (3.25x10-4) and decrease as the stagger angel is increased. When the rotor speed approaches 1700 rpm, the amplitude of vibration appears with large magnitude, but less than that for rotor speed of (1339)rpm .While in y- direction, as shown in figure(18), the amplitude is less in magnitude, but also it is maximum at (1339 rpm), approximately equal to $1x10^{-4}$m . The amplitude increases as the unbalance force increases. However Figure (18) shows that the modulus of the amplitudes increases drastically at and grater than the rotor speed (1700 rpm). These results indicated that the effects of unbalance forces are highly dangerous on the fan system operations and this effect may damage the system.

CONCLOSION REMARKES

Strouhal and Reynolds numbers represents clearly the flow and system frequency characteristics. Vibration response measurements and prediction yield great deal of information concerning any faults within rotating machines. The identification of common mass unbalance by vibration analysis is very well developed and can be performed in many ways. The experimental and the theoretical results are agreed well except one case. The natural frequency occurred in all cases approximately at the same speed in x and y directions.

REFRENCES

Barth & Zsolcsa , K.Paranabesh "Effect of Damping on the Lateral Critical Speed of Rotor-Bearing System" J. of Engineering of Industry V.93 .No. 2,pp(505- 513),May 1976.

Franklyn Kelecy "Study Demonstrates that Simulation can Accurately Predict Fan Performance "Journal Articles By Fluent Software Users. JA 108, pp(1-4),2002.

I, Wattar, W.Hafez, Z.Gao "Model Based Diagnosis of Chaotic Vibration signals", ABB Automatically Cleveland State University, OH.2000

L. Neuhaus and W. Neise "Active Flow Control to Improve the Aerodynamic and Acoustic Performance of Axial Turbo machines" American Institute of Aeronautics and Astronautics, Inc., AIAA, 2948 June 2002.

M. A. Tawfik "Lateral vibration of Branch Systems in Particular Vertical Machines "M.s.c. Thesis, Cranfield Institute of Technology 1978.

M.A.Tawfik;"The effect of Misalignment on the dynamic Performance of the Crank Shaft Bearing System in a Diesel Engine ", PhD Thesis, Mechanical Engineering, University of Technology, Baghdad, October 1996.

McGraw-Hill, "Strouhal Number", Dictionary of Scientific and Technical Term, 2006.

R.N. Peter Childs, "Mechanical Design" John Wily & Sons, Inc. N.Y., Toronto, p16, 1998.

S.L. Dixon, "Fluid Mechanics, Thermodynamics and Turbomachinery", 3ed edition, 1978.

Tohn M.Vance "Rotor Dynamic of Turbomachinary" John Wiley and sons.Inc, 1988.

Yunus A.C. Engel, John M.Cimbala "Fluid Mechanics; Fundamentals and Applications "Mc GRAW Hill, International Edition ,2006

SYMBOLS	DEFINITION	UNITS
[P]	Point matrix	--------
[F]	Field matrix	--------
Re	Reynolds number based on fan diameter	$\frac{\rho U_{\infty} D_f}{\mu}$
St	Strouhal number	$\frac{f D_f}{U_{\infty}}$
U_x ,U_y	Unbalanced forces	kg/m
Ω	Angular speed	rad/s
T	Time	s
[U]	Combined element matrix	-------
$U^{*}x,y$	Unbalance force in x &y directions	kg.m
U_{∞}	Stream velocity	m/s
U	Absolute velocity	m/s
Vz	Axial force in z direction	N
Vx,Vy	Shear force in x &y	N
W	Applied load on bearing	N
W_1	Relative velocity	m/s
X,Y,Z	Deflection in x,y and z direction	m
$[Z]^{L}$	State vector at the left of mass	-------
$[Z]^{R}$	State vector at the right of mass	-------
Z_f	Number of Blade	------
x^{*}, y^{*}	Relative motion in x &y	Mm
Ω	Rotational speed	rpm

Fig.1 Fan Duct System Test Rig assembly

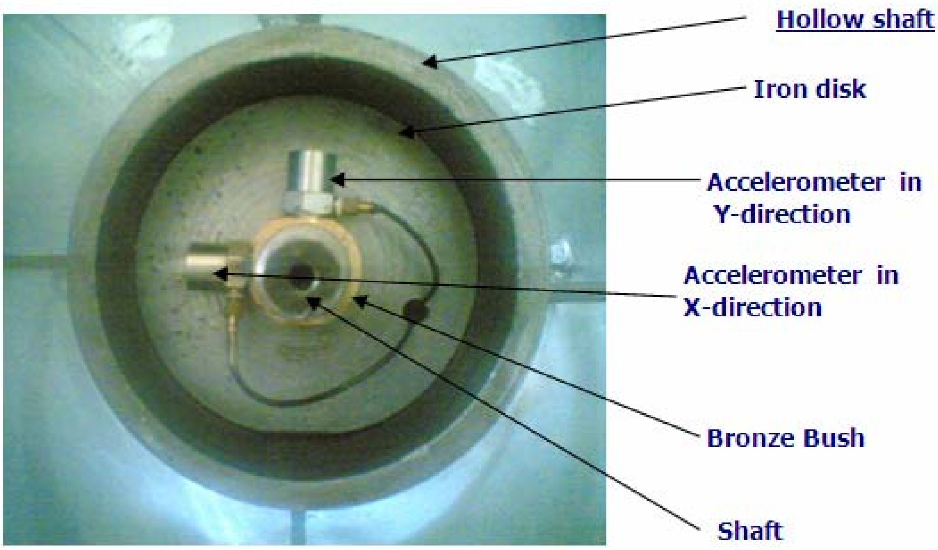

Fig.(2) Two accelerometers mounted on the Bush bearing .

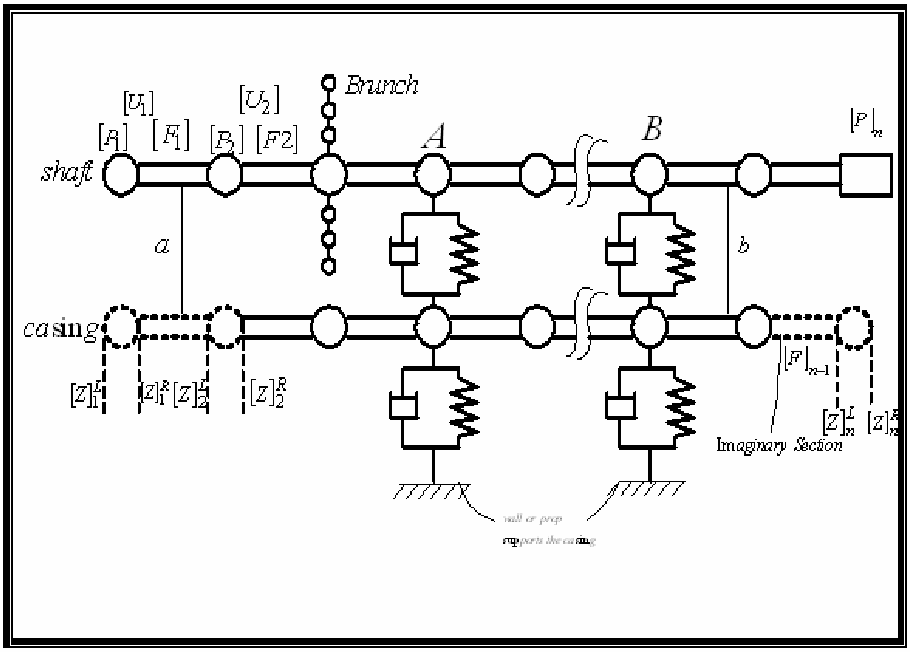

Fig. (3) Mathematical model of horizontal machine, having shaft and casing and indexing of the stations and the corresponding shaft and casing element

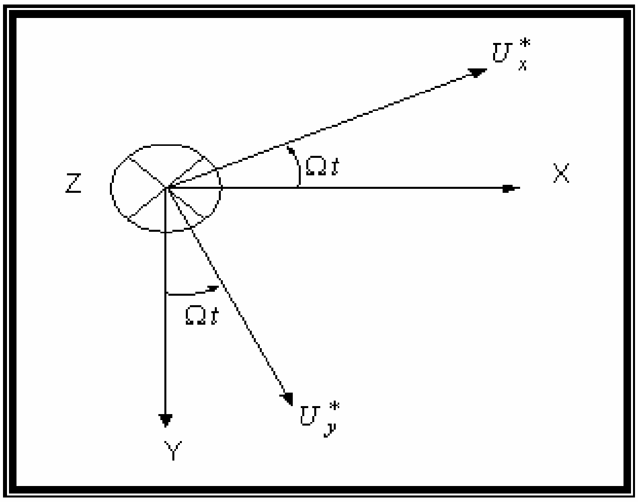

Fig. (4) Unbalance Force Component

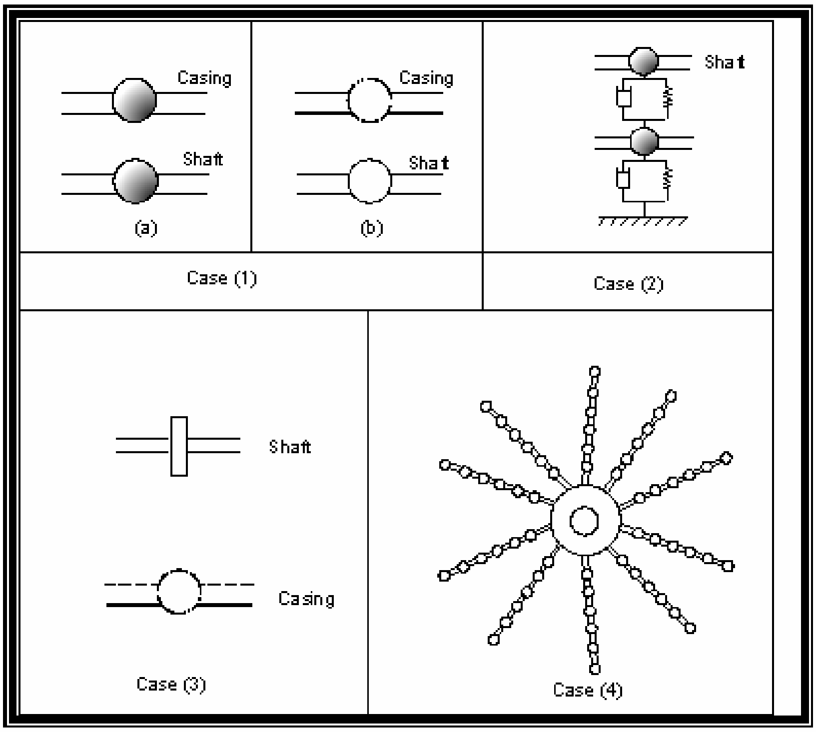

Fig. (5) General Form of Point Matrix of Rotor Casing System.

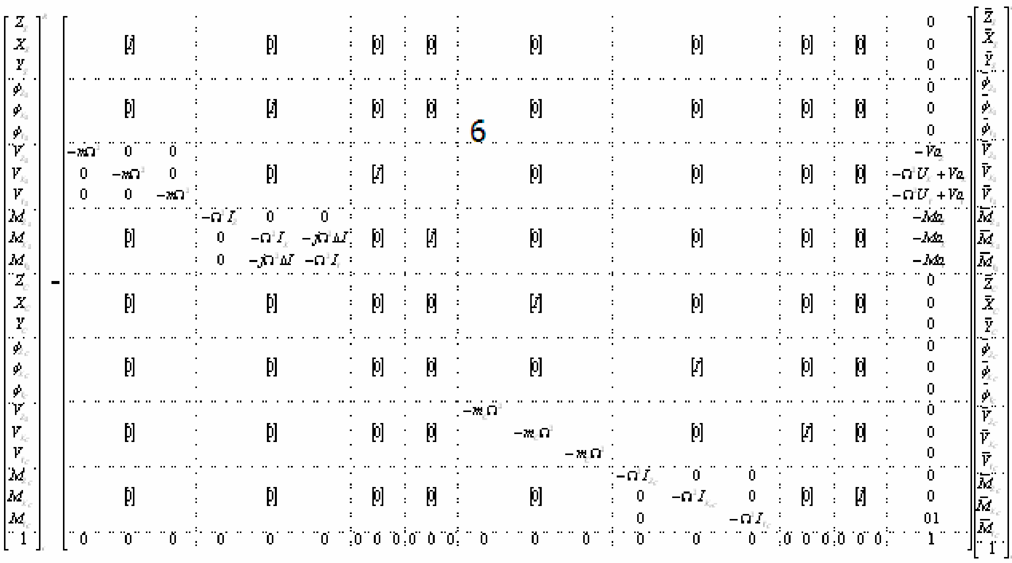

Fig.(6) Point matrix of real masses in shaft and casing .

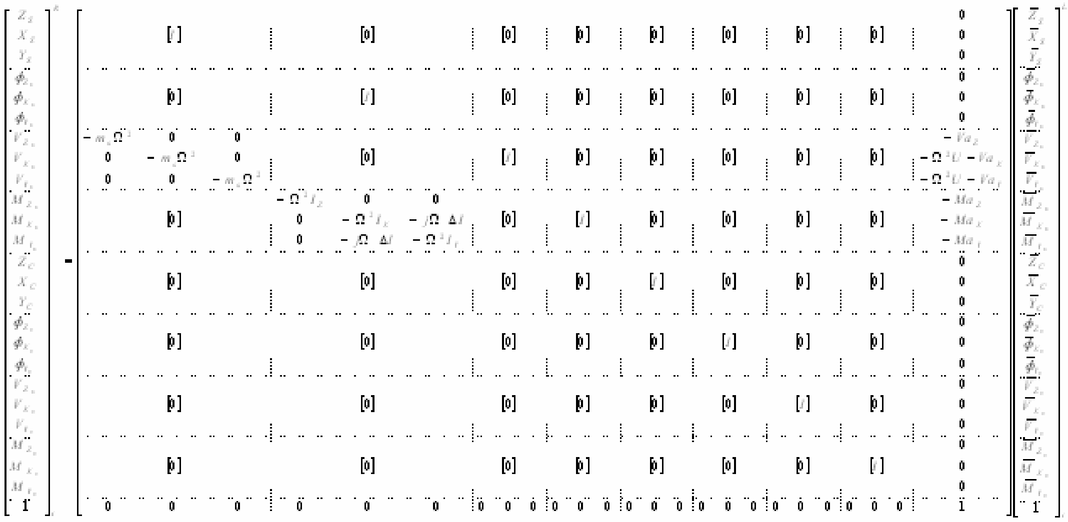

Fig(7)point matrix of real mass of shaft and imaginary part of casing

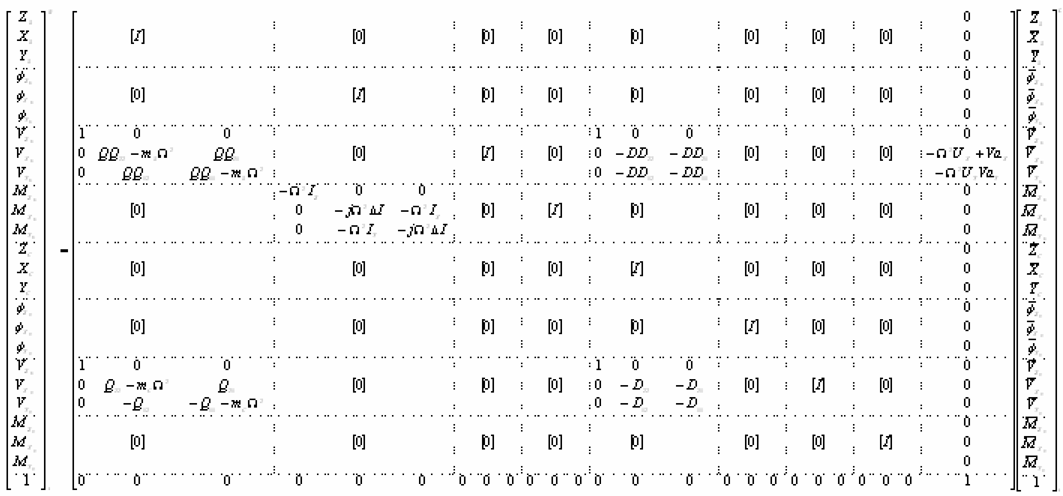

Fig.(8) Point matrix of case (2) Bearing at station considered

$$\begin{bmatrix} Z \\ X \\ Y \\ \phi_Z \\ \phi_X \\ \phi_Y \\ V_Z \\ V_X \\ V_Y \\ M_Z \\ M_X \\ M_Y \\ 1 \end{bmatrix}^R = \left[\begin{array}{cc:c:c:c} [I] & [0] & [0] & [0] & \begin{matrix}0\\0\\0\end{matrix} \\ \hdashline [0] & [I] & [0] & [0] & \begin{matrix}0\\0\\0\end{matrix} \\ \hdashline \multicolumn{2}{c:}{[R_s]-\sum\left[U_{PV}\cdot U^{-1}_{VV}\right]} & \begin{matrix}[I]\\ \\ [0]\end{matrix} & \begin{matrix}[0]\\ \\ [I]\end{matrix} & [R_s]-\sum\left[U_P-U_{PV}\cdot U^{-1}_{VV}\cdot U_V\right] \\ \hdashline \multicolumn{2}{c:}{0\ 0\ 0\ 0\ 0\ 0} & 0\ 0\ 0 & 0\ 0\ 0 & 1 \end{array}\right]^L \begin{bmatrix} \overline{Z} \\ \overline{X} \\ \overline{Y} \\ \overline{\phi}_Z \\ \overline{\phi}_X \\ \overline{\phi}_Y \\ \overline{V}_Z \\ \overline{V}_X \\ \overline{V}_Y \\ \overline{M}_Z \\ \overline{M}_X \\ \overline{M}_Y \\ 1 \end{bmatrix}_i$$

Fig. (9) Point matrix of the brunch system.

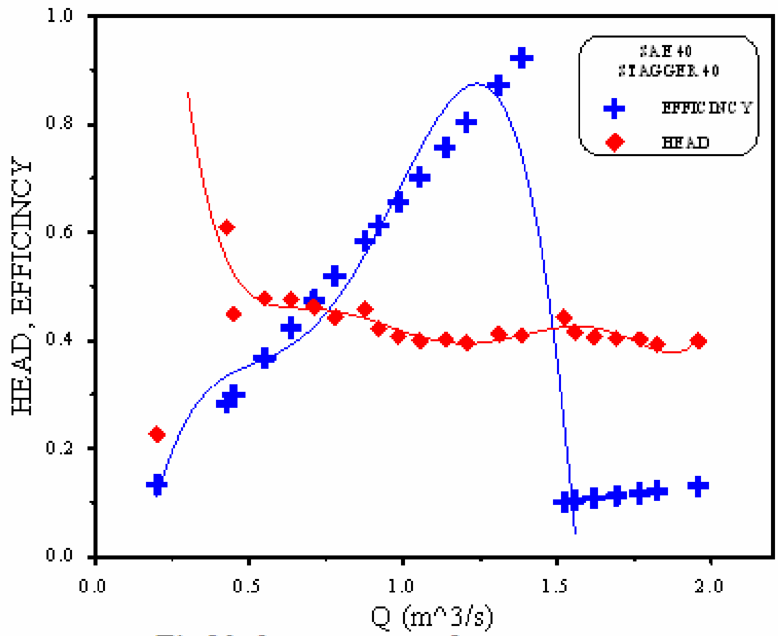

Fig.10 fan system performance

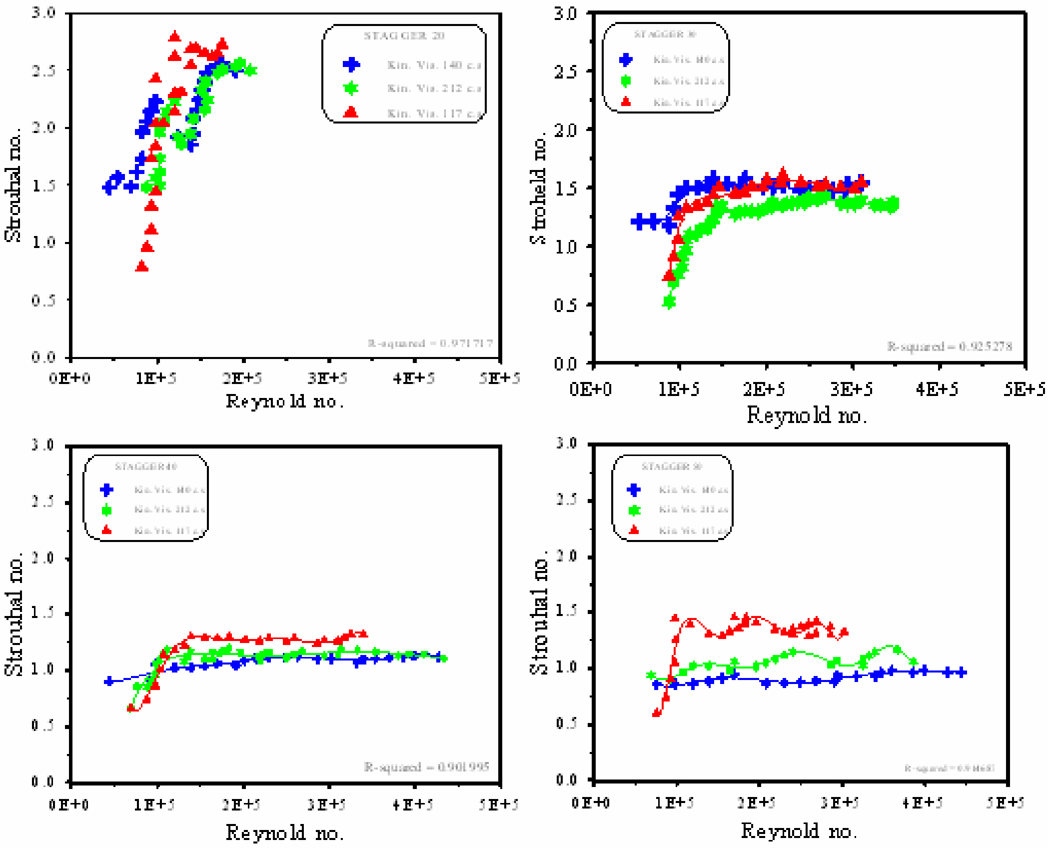

Fig. (11) St Verses Re for various oil kinematics viscosity and fan blade stagger angle.

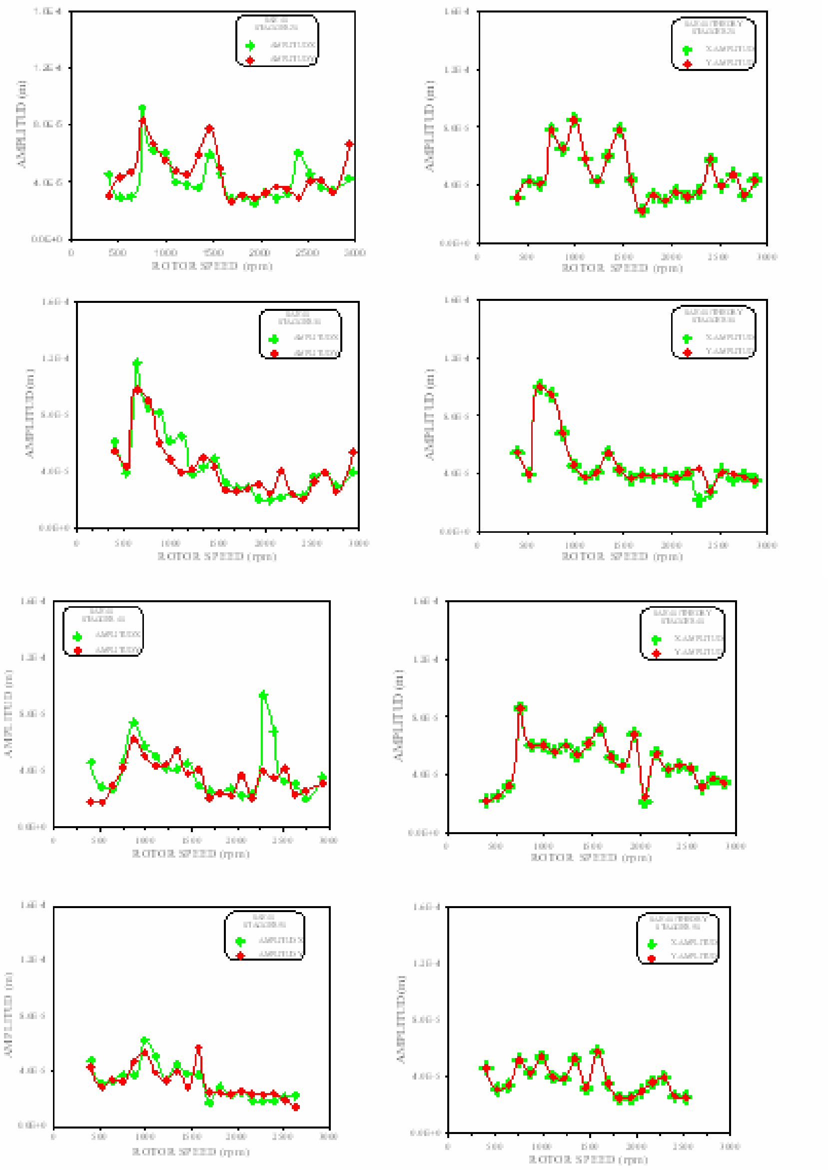

Experiment Theory

Fig.12 Experimental and Theoretical Amplitude in X and Y Direction versus Rotor Speed for SAE 40 Kin. Vis.=140 c.s.

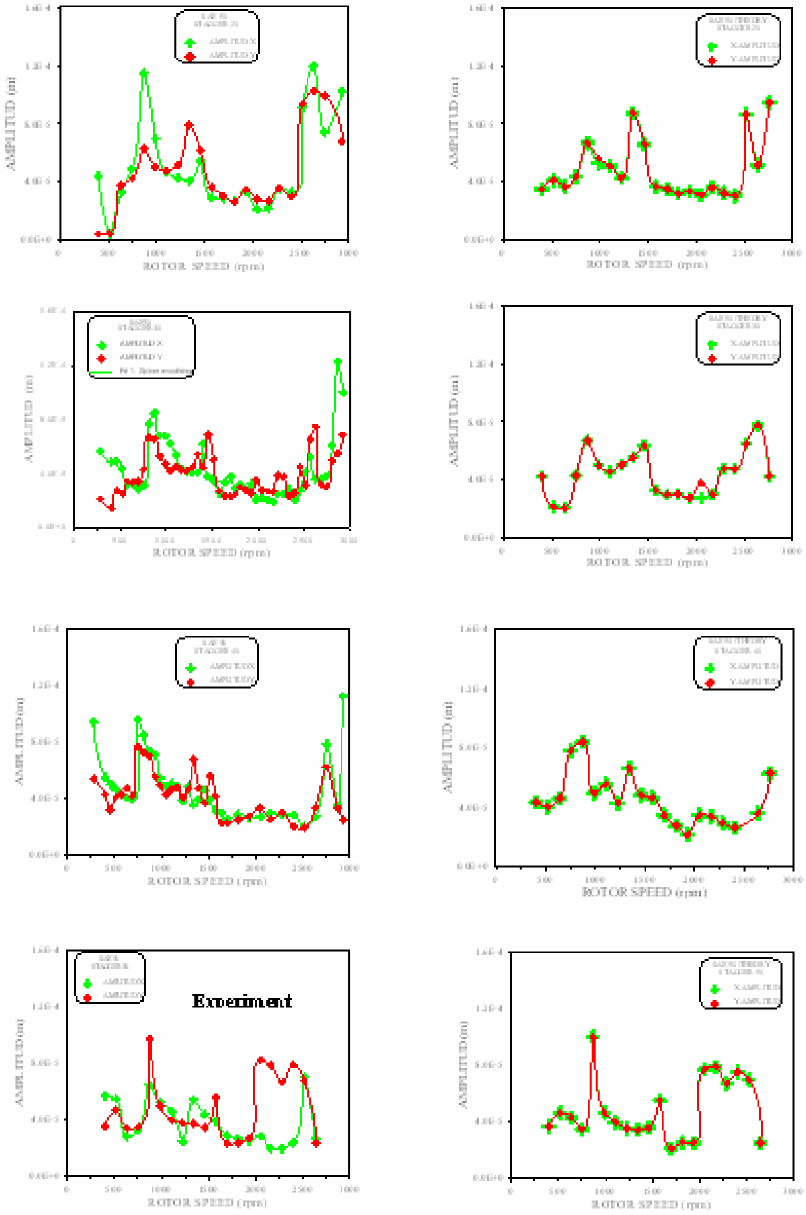

Experiment Theory
Fig.13 Experimental and Theoretical Amplitude in X and Y Direction versus Rotor Speed for SAE 50 Kin. Vis.=212 c.s.

Fig.14 Experimental and Theoretical Amplitude in X and Y Direction versus Rotor Speed for Degraded Oil SAE 40 Kin. Vis.=117 c.s.

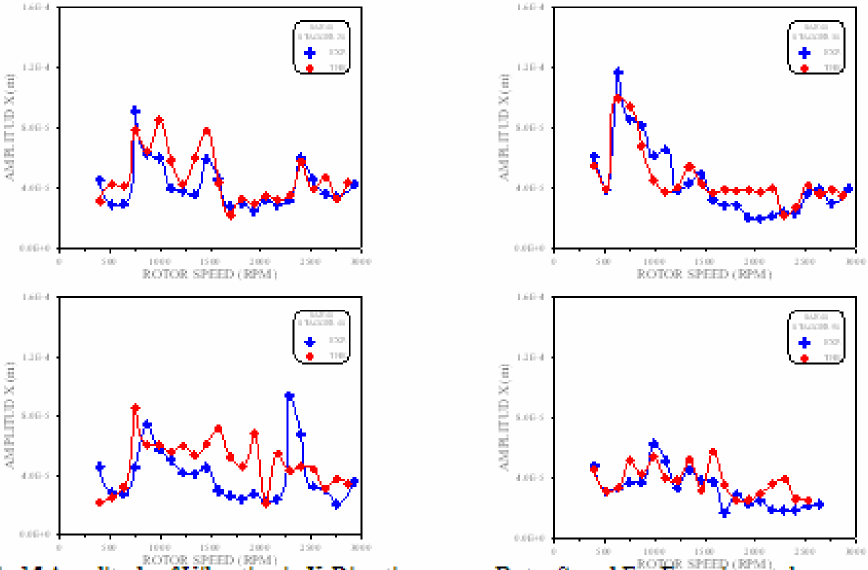

Fig.15 Amplitude of Vibration in X-Direction versus Rotor Speed For Experimental and Theoretical work for Different values of Stagger Angle and for Constant value of Viscosity SAE 40

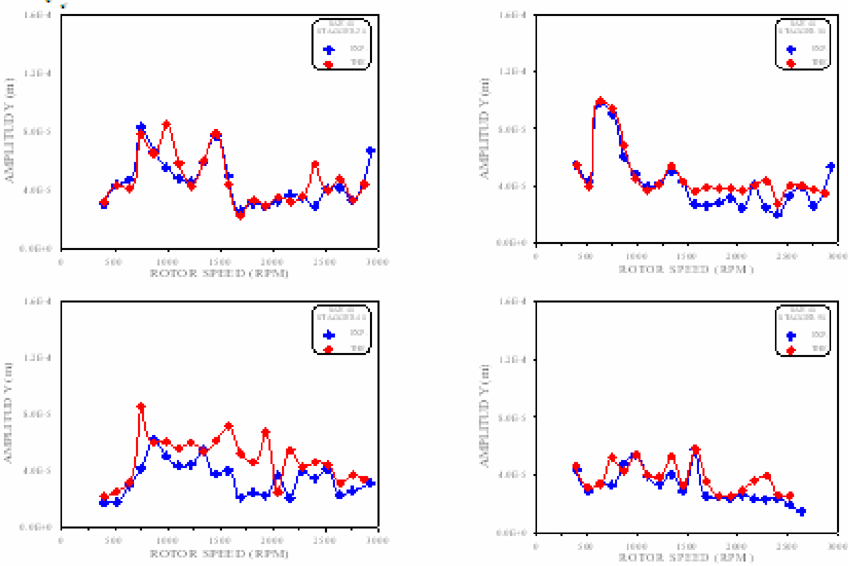

Fig.16 Amplitude of Vibration in Y-Direction versus Rotor Speed For Experimental and Theoretical work for Different values of Stagger Angle and for Constant value of Viscosity SAE 40

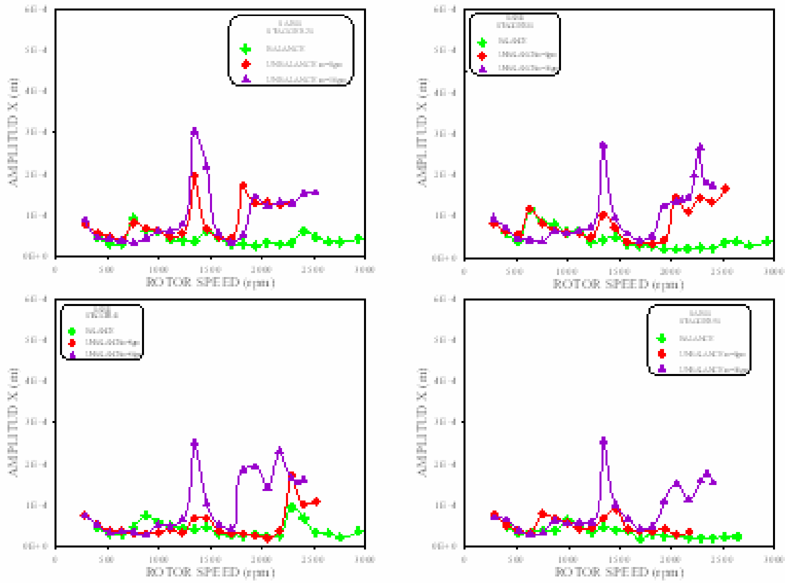

Fig. 17 Amplitude of Vibration in X-Direction versus Rotor Speed at Different Unbalance Force and Stagger Angle for SAE 40(Kin. Vis.=140 c.s.)

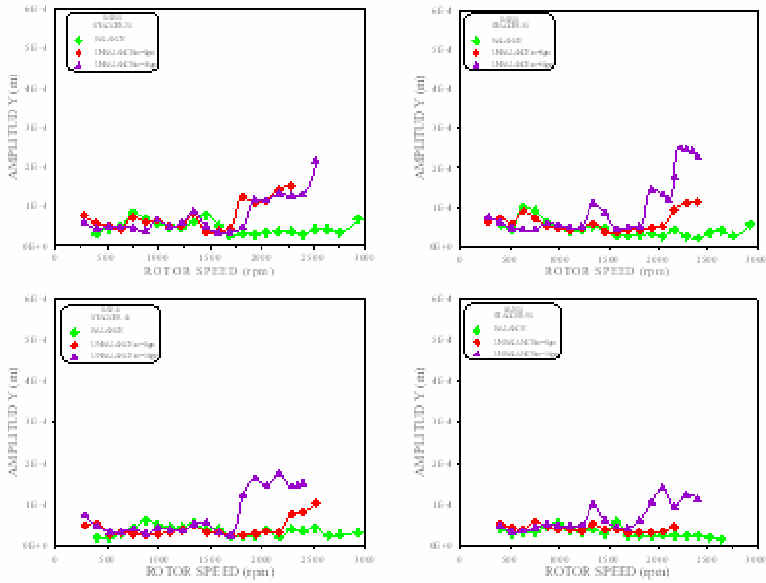

Fig. 18 Amplitude of Vibration in Y-Direction versus Rotor Speed At Different Unbalance Force and Stagger Angle for SAE 40 (Kin. Vis.=140 c.s.)